Article

A Feasibility Study on Timber Damage Detection Using Piezoceramic-Transducer-Enabled Active Sensing

Jicheng Zhang [1], Yongshui Huang [1] and Yu Zheng [2],*

[1]   School of Urban Construction, Yangtze University, Jingzhou 434023, China; 100995@yangtzeu.edu.cn (J.Z.); 201672324@yangtzeu.edu.cn (Y.H.)

[2]   School of Environment and Civil Engineering, Dongguan University of Technology, Dongguan 523808, China

*   Correspondence: zhengy@dgut.edu.cn

Abstract: In recent years, piezoelectric-based transducers and technologies have made significant progress towards structural health monitoring and damage evaluation for various metal and concrete structures. Timber is still commonly used as a construction material in practical engineering; however, there is a lack of research on the health monitoring of timber-based structures using piezoelectric-based transducers and methods. This paper conducts a feasibility study on timber damage detection using surface-mounted piezoelectric patches, which enable the stress-wave-based active sensing approach. Typical damage modes in timber frame structures, such as surface cracks and holes, were investigated in this study. In the active sensing approach, one piezoceramic transducer is used as an actuator to generate stress waves, which propagate along the surface of the timber structure, and other piezoceramic transducers function as sensors to detect the propagating stress waves. Defects, such as a crack or a hole, induce additional attenuation to the propagating stress wave. Based on this attenuation, the proposed method can detect the defects using the wavelet-packet-based damage index, demonstrating its implementation potential for real-time timber damage detection.

Keywords: timber damage detection; piezoelectric transducer; active sensing approach; wavelet-packet-based damage index

1. Introduction

Nowadays, timber is one of the most common construction materials for wood-framed houses [1]. However, timber structures are susceptible to termite attacks, fungal decays, and cracks during their service life due to mechanical loads and environmental effects. It has become increasingly evident that those defects have been major factors in the deterioration of timber structures. These damages in timber structures, if not detected at the earliest possible stage, can weaken their structural loading capacity and shorten their service life. The study of timber damage detection is of great significance to reducing maintenance costs and ensuring structural safety [2].

With the recent rapid advances in structural health monitoring [3–6] and damage detection technology [7,8], damage detection on timber and wood structures has received increasing attention from researchers over the past decades. Peterson et al. [9,10] and Hu et al. [11] developed statistical algorithms and damage indices by computing the mode shapes of timber beams before and after damage under vibration tests. Subsequently, Choi et al. [12] proposed an improved damage detection algorithm to estimate the status of wooden material by comparing the modal strain energy derived from the first two flexural vibration modes. Similarly, the wavelet transform method [13], the transfer

function method [14,15], and the mode shape reconstruction technique [16] were adopted to find the model shapes of timber, which revealed that the mode shapes before and after damage could be further utilized to identify the damage status and location in timber. However, it is difficult to establish real-time monitoring by using such vibration-based methods since external excitations are required in these methods.

Recently, a few real-time methods for timber damage detection have been reported in the literature. Annamdas et al. [17,18] and Wang et al. [19] utilized the piezoelectric impedance method to detect the different types of damage on timber and to evaluate its health condition. Sanabria et al. [20] assessed the bonding quality of glued timbers, and the presence of glue by using the air-coupled ultrasound (ACU) inspection method. Similarly, another ultrasonic testing method was developed by Concu et al. [21] to detect the adhesion status and damage in cross-laminated timber (CLT). By measuring the velocity of ultrasound waves in the wave path perpendicular to the timber plane, the health condition of CLT can be determined. Peterson et al. [22] proposed a combined structural dynamic excitation system and ultrasonic inspection approach to evaluate the integrity of timber bridges. Ross et al. [23] verified the effectiveness of the stress wave method in monitoring a timber bridge by estimating the moisture and decay condition in the wood. In addition, Dackermann et al. [24] proposed a detailed measuring procedure for assessing structural timber by using the stress wave method. By measuring the time of flight (TOF) when the wave propagates across the timber, the moisture condition, decay status, and the effect of annual growth rings can be obtained.

Lead Zirconate Titanate (PZT) is a commonly used piezoceramic material with the advantages of low cost, fast response [25], embeddability [26–29], strong piezoelectric effect [30], dual ability of actuation and sensing [31,32], wide bandwidth [33], and energy harvesting capacity [34,35]. Due to its wide bandwidth, PZT is often used for stress wave generation [36,37] and detection [38–40]. The PZT-enabled active sensing approach using surface-mounted or embedded transducers has shown great potential for the structural health monitoring of mechanical and civil structures in real time [41–46]. The principle of this approach is to measure the propagating wave property changes due to the structural damage by using a pair of PZT transducers or a deployed sensor network. An increasing amount of research on structural health monitoring using the active sensing approach has been conducted and reported, including crack and corrosion detection of a metal pipeline system [47,48], monitoring of bolt and rock bolt looseness [49–52], damage identification in space structures [53], crack and leakage detection of concrete structures [54,55], bond slip detection of composite concrete structures [56–59], early-age cement hydration monitoring [60–62], nondestructive concrete strength evaluation [63], and disbond detection in adhesively bonded structures [64,65]. Moreover, Park et al. [66] proposed a self-powered flexible piezoelectric pulse sensor based on a PZT thin film for a real-time health care monitoring system. Jeonget al. [67] proposed a high-performance (K,Na)NbO3 (KNN)-based flexible piezoelectric energy harvester (f-PEH) using the aerosol deposition method (ADM) with the laser lift-off (LLO) process and conducted experimental tests of cell viability and histological stability to investigate the biocompatibility of both KNN and PZT. However, the study of damage detection methods of timber or timber-supported structures based on the active sensing approach using PZT transducers is still rather limited.

In this paper, a feasibility study on timber damage detection using the PZT-transducer-enabled active sensing approach was investigated. In this investigation is an attempt to employ a stress-wave-based active sensing approach to monitor the cracks and holes in a timber structure. For each timber specimen, one PZT was used as an actuator, which generated guided stress waves to the other PZT that was used as a sensor. Since the stress wave propagation is highly sensitive to the defects on the wave path, timber surface damage such as a crack or a hole can attenuate the stress wave energy. A wavelet-packet-based damage index was applied to characterize the damage severity based on the attenuation ratio of the received wave energy. The analytical results indicated that this damage index had the capability of evaluating crack depths, hole depths, and hole sizes quantitatively and accurately.

2. Principles

2.1. Active Sensing Approach

To monitor time damage using a stress-wave-based active sensing approach, detection equipment was established in this study as shown in Figure 1. Figure 1 demonstrates the principle of this approach to monitor a crack and a hole on a timber beam. It can be seen that a pair of PZT patches (one as an actuator coded as PZT1 and the other as a sensor coded as PZT2) are surface-bonded on a timber specimen to generate and receive stress waves, respectively. When a crack or a hole occurs on the timber surface, the propagating wave energy is reduced by the wave reflection from the defects. This leads to a decreased signal received by the PZT sensors compared to that across an intact timber surface. Additionally, increasing the damage level correspondingly results in a lower received wave energy; damage increase includes increases in crack depth, hole size, and hole depth. In order to quantitatively evaluate the damage severity, a wavelet-packet-based damage index was adopted, which is presented and discussed the next section.
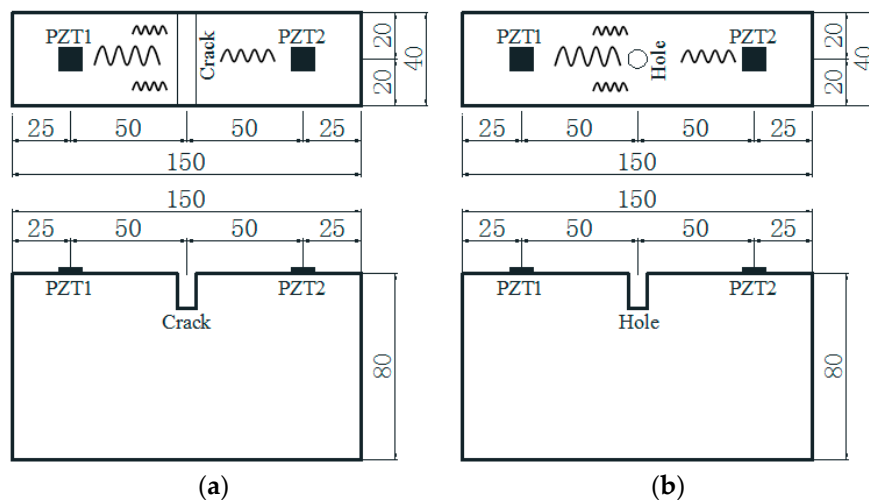

Figure 1. Stress-wave-based active sensing approach for timber damage detection (unit: mm). (**a**) Timber damage with a crack; (**b**) timber damage with a hole.

2.2. Wavelet-Packet-Based Damage Index

Wavelet packet analysis is a linear time–frequency analysis method with good time–frequency positioning characteristics, which can effectively decompose a variety of time-varying signals. The wavelet-packet-based approach has been widely used in engineering structural analysis [68–71]. In this investigation, a wavelet-packet-based damage index was used to evaluate the timber damage severity. The procedure of establishing the damage index is as follows:

Firstly, the received signal at the ith measurement, $\mathbf{S}_i$, is decomposed by a 5-level wavelet packet decomposition into 2^5 signal subsets with different frequency bands. The mother wavelet used in this research is "db2". The signal subset $\mathbf{X}_{i,j}$, where j is the frequency band ($j = 1, 2, \ldots, 2^5$), can be expressed as

$$\mathbf{X}_{i,j} = \left\{ X_{i,j,1}, X_{i,j,2}, \ldots, X_{i,j,m} \right\} \tag{1}$$

where m is the number of data samplings of the decomposed signal subset.

Secondly, the energy of the signal subset, $E_{i,j}$, can be defined as

$$E_{i,j} = X_{i,j,1}^2 + X_{i,j,2}^2 + \ldots X_{i,j,m}^2 \tag{2}$$

Finally, the damage index *I* is defined using the root-mean-square deviation (RMSD), and it can be given as

$$I(i) = \sqrt{\frac{\sum_{j=1}^{25} \left(E_{i,j} - E_{1,j}\right)^2}{\sum_{j=1}^{2^n} E_{1,j}^2}} \tag{3}$$

where $E_{1,j}$ of the signal $\mathbf{S_1}$ refers to the signal that is measured when the structure is healthy. It is clear that the minimum value of the damage index is 0 when there is no damage, as compared with the baseline value, and the maximum value is 1 when the damage is so severe that the sensor receives no signal. It should be noted that a baseline signal response (healthy condition) is always required for this approach. When the baseline signal response (healthy condition) is measured, the RMSD value at the healthy condition is always 0. All the other signal responses measured in damaged conditions are compared to that measured in the healthy condition.

3. Experimental Setup

3.1. Timber Specimens

A total of six timber specimens (pine wood from North America) with the same dimensions were prepared in this experimental test. The dimensions of each test specimen were 0.04 m wide by 0.15 m long and 0.08 m deep. For each specimen, two PZT patches were mounted at the predetermined locations using epoxy (Loctite Heavy Duty 5 min epoxy), as shown in Figure 2. Thus, a thin layer of epoxy exists as the interface between the PZT and the wooden surface. In this research, the PZT sensor was purchased from Beijing Ultrasonic. The PZT sensor is a sandwiched structure with two electrode layers and one layer of PZT material. The dimensions of the PZT sensor are 10 mm in diameter and 0.2 mm in thickness. The six specimens were placed in three groups. It is illustrated in Figure 2 that some artificial structural damages were applied in all the test specimens before monitoring. For Group A (Specimens 1 and 2), a crack was cut on each specimen. For Group B (Specimens 3 and 4) and Group C (Specimens 5 and 6), a hole was drilled in each specimen. The location of the PZT patches and preconfigured damage are presented in Figure 2.
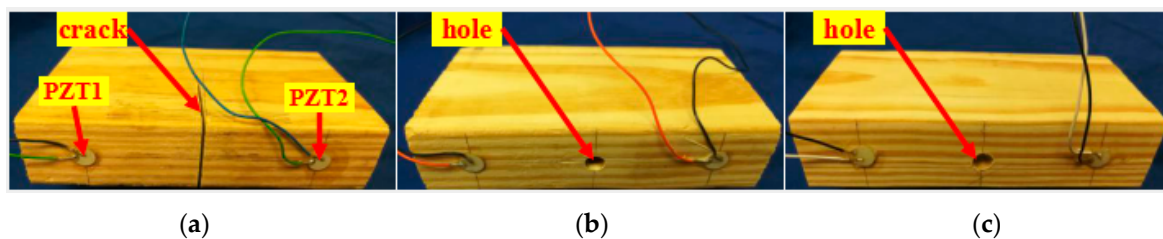

(a)　　　　　　　　　　　　　**(b)**　　　　　　　　　　　　　**(c)**

Figure 2. Timber specimens for different groups. (**a**) Specimen of Group A; (**b**) specimen of Group B; (**c**) specimen of Group C.
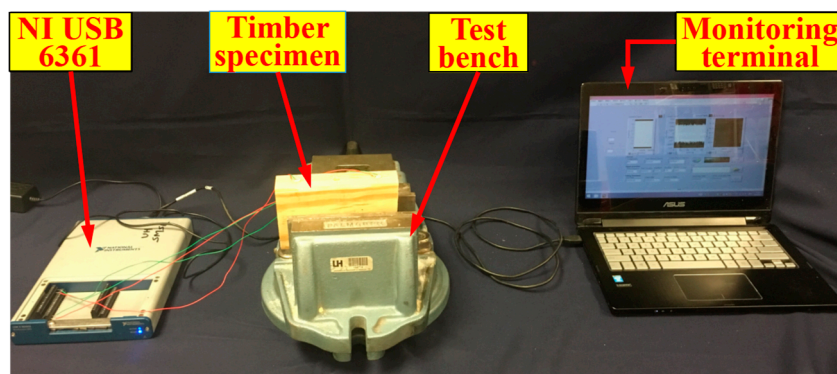
In this study, three different damage types including crack depth, hole depth, and hole size (diameter) were investigated in Groups A, B, and C, respectively (see Table 1). In Group A, cracking damage depths were varied over eight sizes: 0, 2, 4, 6, 8, 10, 20 and 40 mm. The width of the crack was set at 1.5 mm for all test models. For Group B, the effect of hole depth was investigated by varying the structural parameter from 0 to 40 mm over eight steps (see Table 1). The diameter of the hole was fixed at 4 mm for all the models in this group. Finally, five test specimens with different hole diameters were conducted in Group C (see Table 1). This structural variable was varied from 0 to 9 mm to investigate the effect of this structural defect. For the specimens in this group, the depth of the hole was selected to be 4 mm. Table 1 depicts the investigated damage status of all the test specimens in this study.

Table 1. Test cases of specimens in Groups A, B, C.

Group A	Case	1	2	3	4	5	6	7	8
	Crack depth (mm)	0	2	4	6	8	10	20	40
Group B	Case	1	2	3	4	5	6	7	8
	Hole depth (mm)	0	2	4	6	8	10	20	40
Group C	Case	1	2	3	4	5			
	Hole diameter (mm)	0	3	5	7	9			

3.2. Experimental Setup and Experimental Procedure

Figure 3 shows the experimental setup, including a data acquisition system (NI USB-6361) with a laptop and a timber specimen fixed on a bench. The sampling frequency of the data acquisition system is 2 MS/s. For each case, the PZT actuator was excited by a swept sine wave signal generated guided stress wave from one side of the timber specimen. The PZT sensor recorded the response signal from the other side. The start frequency, stop frequency, amplitude, and period of the excitation signal were 100 Hz, 300 kHz, 10 V, and 1 s, respectively. The frequency step used in this research was 50,000. To minimize the influence of the environmental humidity on the results, all the tests were done within 2 h in the laboratory. The humidity and temperature change within these two hours can be ignored.

Figure 3. Experimental setup.

4. Results and Discussion

The time domain signal responses of the PZT sensors of Groups A, B, and C are given in Figures 4–6, respectively. Each curve is one period of the sensor signal response of the swept sine wave signal, which is 1 s in the time domain. Due to different damage modes, the received signal of the PZT sensors from different groups is also diverse. In addition, compared to the two specimens with the same damage status in each group, it can be seen that the received signal still presented a unique characteristic. This could be due to the differences among the timber specimens, epoxy dimensions, and PZT wire welding. In the study of a general trend in the signal response of all the test specimens, it was shown that a reduction in the received signal indicated an increase in the timber damage severity. Increasing the cracking depth, hole depth, or hole diameter resulted in significantly smaller stress wave propagation energy on the timber structure. Interestingly, the received signal of Case 8 from Group A is much less than those of Case 8 from Group B and Case 5 from Group C. The reason for this is that deep crack damage across the wave path attenuates much more energy than hole damage.
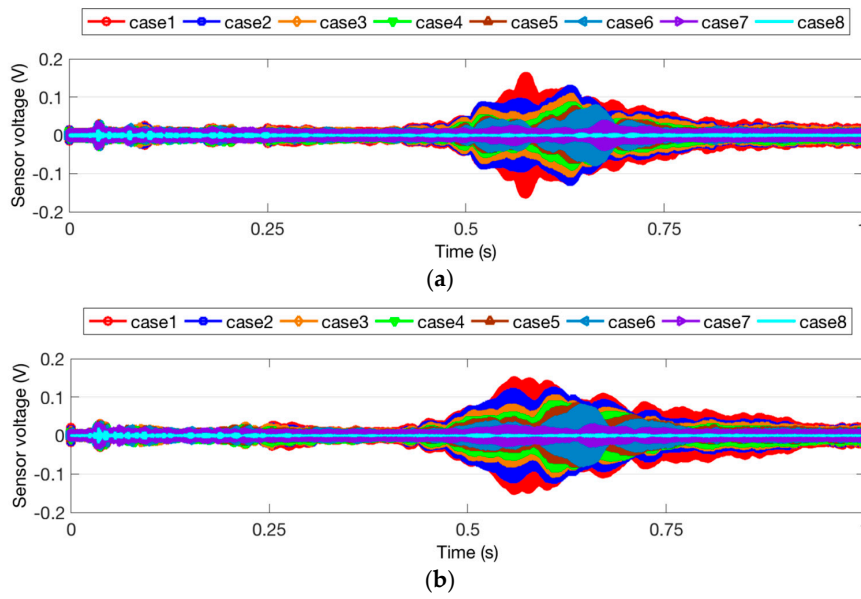
Figure 4. Sensor signal response for Group A. (**a**) Specimen 1; (**b**) Specimen 2.
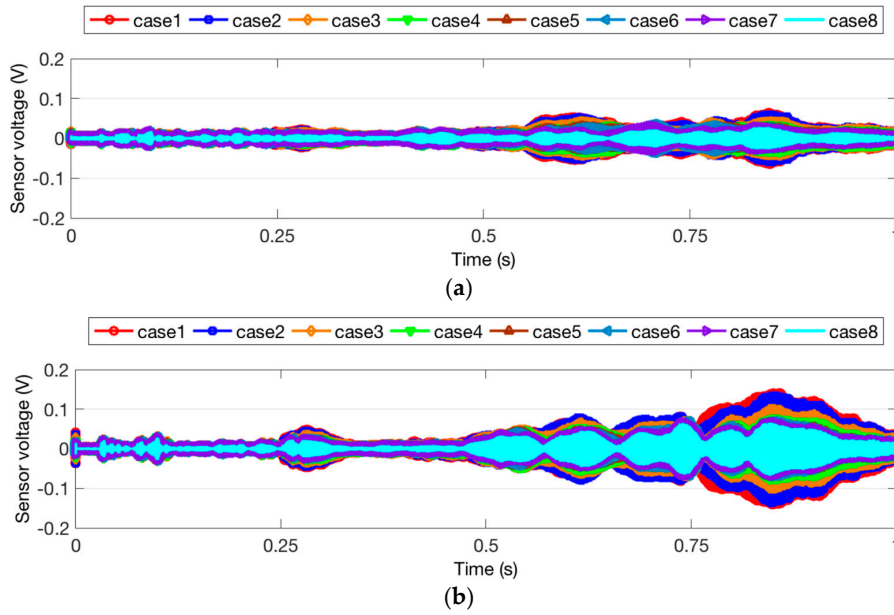

Figure 5. Sensor signal response for Group B. (**a**) Specimen 3; (**b**) Specimen 4.
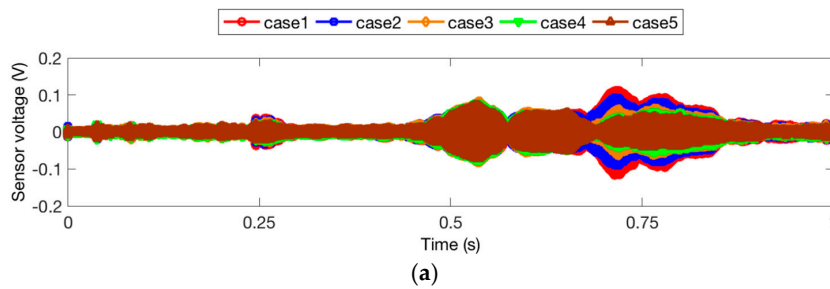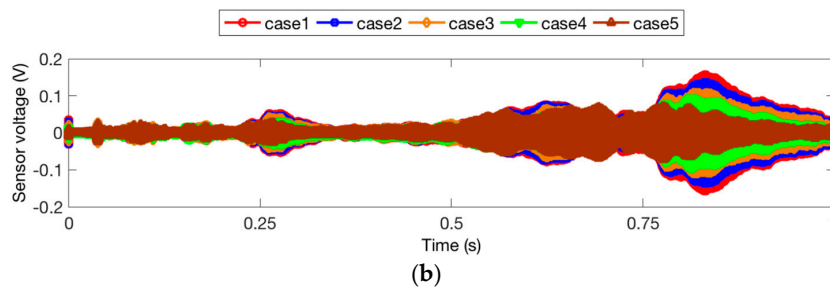

Figure 6. *Cont.*

(b)

Figure 6. Sensor signal response for Group C. (**a**) Specimen 5; (**b**) Specimen 6.

Additionally, in order to quantitatively evaluate the loss of the stress wave energy, the wavelet-packet-based energy indices for all the groups were calculated based on Equations (1)–(3). The results of those indices are shown in Figures 7–9. Compared to the time domain signal response, those damage indices show promise for estimating the damage severity. In addition, though the time domain signal responses of the two specimens from the same group are different, the values of their damage indices are close to each other. This means that the wave attenuation ratio of the same types of damage is almost the same. As shown in Figures 7 and 8, the damage indices in some cases—Cases 7 and 8 from Group A; Cases 5, 6, 7, and 8 from Group B—reached a constant value, which indicated that the wave attenuation could reach maximum when the crack and hole are at certain depths. In addition, as shown in the damage index (Figures 7–9), with the increase of the damage severity, the value of the index correspondingly increases. When the value of the index approaches 1, it means that the structure is subject to severe damage. In the real case, the proposed damage index could provide an early warning for early age damage initiation, as well as a warning when the structure is under severe damage conditions.
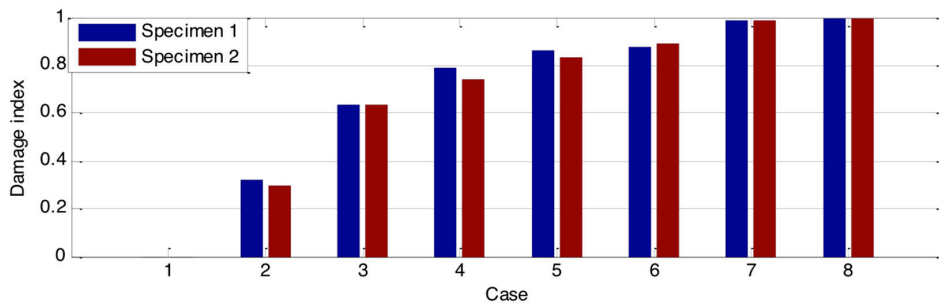

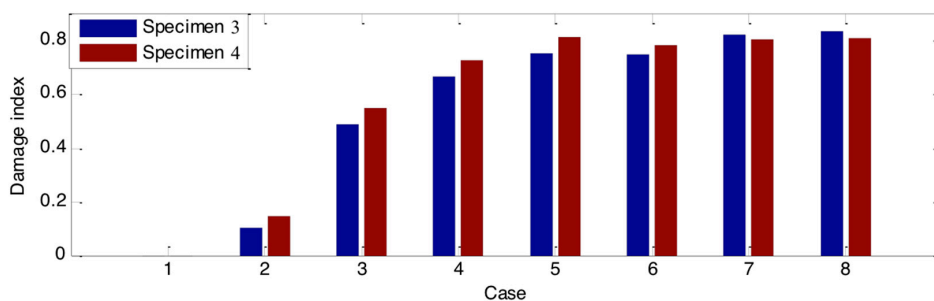**Figure 7.** Damage indices of timber with different crack depths.

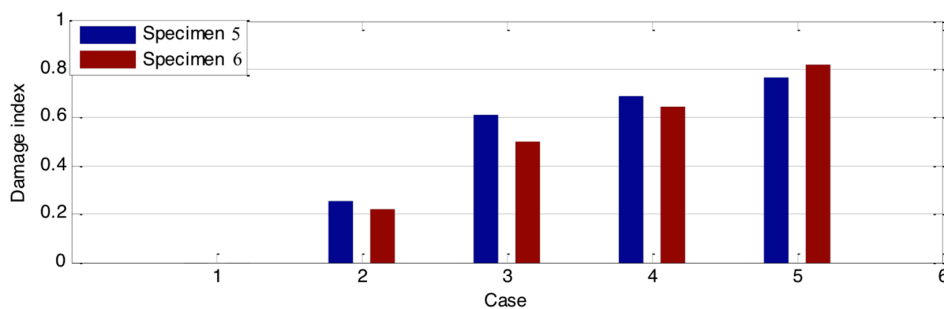**Figure 8.** Damage indices of timber with different hole depths.

Figure 9. Damage indices of timber with different hole diameters.

The experimental results revealed that the stress-wave-based active sensing approach has great potential to monitor the damage in timber structures. However, there are still many challenges for practical applications using this method. Firstly, the damage mode in timber structures still cannot be identified using these methods, although the structural damage in timber can be detected by the time domain signal responses and wavelet-packet-based damage indices. Secondly, some factors, have not been considered in this research, including humidity, boundary condition, epoxy influences, temperature, wood type, wood size, etc., which could affect the monitoring results. Further research works should be carried in the future to clarify these issues. Finally, another commonly used method called the correlation coefficient deviation metric (CCDM) should be compared with the RMSD method for the structural health monitoring of timber damage.

5. Conclusions and Future Work

This research is the first attempt to use a stress-wave-based active sensing approach and a wavelet-packet-based damage index for timber damage monitoring. Two typical types of damage—cracks and holes—were used in this study. The effects of crack depth, hole depth, and hole diameter were investigated by varying those variables. A decreasing trend of the signal amplitude was clearly obtained due to an increase in timber damage. In addition, the damage index values offered a quantitative assessment of the damage severity. The experimental results revealed that this approach could be a promising tool to conduct real-time monitoring of timber damage. To develop further study of this novel monitoring method, the application of a stress-wave-based active sensing approach and a wavelet-packet-based damage index for large-scale timber framing structures with damage will be investigated. In addition, the influences of some variables, such as environmental humidity, boundary condition, epoxy, and temperature, will be considered and investigated comprehensively.

Conflicts of Interest: The authors declare no conflict of interest.

References

1. Moody, R. Timber bridges—A rebirth. *Woodl. Manag.* **1994**, *15*, 18–20.
2. Liu, H.; Koyama, C.; Zhu, J.; Liu, Q.; Sato, M. Post-Earthquake Damage Inspection of Wood-Frame Buildings by a Polarimetric GB-SAR System. *Remote Sens.* **2016**, *8*, 935. [CrossRef]
3. Song, G.; Wang, C.; Wang, B. Structural Health Monitoring (SHM) of Civil Structures. *Appl. Sci.* **2017**, *7*, 789. [CrossRef]
4. Yang, Y.; Divsholi, B.S.; Soh, C.K. A reusable PZT transducer for monitoring initial hydration and structural health of concrete. *Sensors* **2010**, *10*, 5193–5208. [CrossRef] [PubMed]

5. Yan, S.; Ma, H.; Li, P.; Song, G.; Wu, J. Development and Application of a Structural Health Monitoring System Based on Wireless Smart Aggregates. *Sensors* **2017**, *17*, 1641. [CrossRef] [PubMed]

6. Duan, W.H.; Wang, Q.; Quek, S.T. Applications of piezoelectric materials in structural health monitoring and repair: Selected research examples. *Materials* **2010**, *3*, 5169–5194. [CrossRef] [PubMed]

7. Broda, D.; Staszewski, W.J.; Martowicz, A.; Uhl, T.; Silberschmidt, V.V. Modelling of nonlinear crack–wave interactions for damage detection based on ultrasound—A review. *J. Sound Vib.* **2014**, *333*, 1097–1118. [CrossRef]

8. Hu, X.; Zhu, H.; Wang, D. A study of concrete slab damage detection based on the electromechanical impedance method. *Sensors* **2014**, *14*, 19897–19909. [CrossRef] [PubMed]

9. Peterson, S.T.; McLean, D.I.; Symans, M.D.; Pollock, D.G.; Cofer, W.F.; Emerson, R.N.; Fridley, K.J. Application of dynamic system identification to timber beams. I. *J. Struct. Eng.* **2001**, *127*, 418–425. [CrossRef]

10. Peterson, S.T.; McLean, D.I.; Symans, M.D.; Pollock, D.G.; Cofer, W.F.; Emerson, R.N.; Fridley, K.J. Application of dynamic system identification to timber beams. II. *J. Struct. Eng.* **2001**, *127*, 426–432. [CrossRef]

11. Hu, C.; Afzal, M.T. A statistical algorithm for comparing mode shapes of vibration testing before and after damage in timbers. *J. Wood Sci.* **2006**, *52*, 348–352. [CrossRef]

12. Choi, F.C.; Li, J.; Samali, B.; Crews, K. Application of modal-based damage-detection method to locate and evaluate damage in timber beams. *J. Wood Sci.* **2007**, *53*, 394–400. [CrossRef]

13. Hu, C.; Afzal, M.T. A wavelet analysis-based approach for damage localization in wood beams. *J. Wood Sci.* **2006**, *52*, 456–460. [CrossRef]

14. Yang, X.; Ishimaru, Y.; Iida, I.; Urakami, H. Application of modal analysis by transfer function to nondestructive testing of wood I: Determination of localized defects in wood by the shape of the flexural vibration wave. *J. Wood Sci.* **2002**, *48*, 283–288. [CrossRef]

15. Yang, X.; Amano, T.; Ishimaru, Y.; Iida, I. Application of modal analysis by transfer function to nondestructive testing of wood II: Modulus of elasticity evaluation of sections of differing quality in a wooden beam by the curvature of the flexural vibration wave. *J. Wood Sci.* **2003**, *49*, 140–144. [CrossRef]

16. Choi, F.C.; Li, J.; Samali, B.; Crews, K. An experimental study on damage detection of structures using a timber beam. *J. Mech. Sci. Technol.* **2007**, *21*, 903–907. [CrossRef]

17. Annamdas, V.G.M.; Annamdas, K.K.K. Impedance based sensor technology to monitor stiffness of biological structures. In *Advanced Environmental, Chemical, and Biological Sensing Technologies VII*; International Society for Optics and Photonics: Bellingham, WA, USA, 2010.

18. Annamdas, K.K.K.; Annamdas, V.G.M. Piezo impedance sensors to monitor degradation of biological structure. In *Advanced Environmental, Chemical, and Biological Sensing Technologies VII*; International Society for Optics and Photonics: Bellingham, WA, USA, 2010.

19. Wang, D.; Wang, Q.; Wang, H.; Zhu, H. Experimental study on damage detection in timber specimens based on an electromechanical impedance technique and RMSD-based mahalanobis distance. *Sensors* **2016**, *16*, 1765. [CrossRef] [PubMed]

20. Sanabria, S.J.; Mueller, C.; Neuenschwander, J.; Niemz, P.; Sennhauser, U. Air-coupled ultrasound as an accurate and reproducible method for bonding assessment of glued timber. *Wood Sci. Technol.* **2011**, *45*, 645–659. [CrossRef]

21. Concu, G.; Fragiacomo, M.; Trulli, N.; Valdès, M. Non-destructive assessment of gluing in cross-laminated timber panels. *WIT Trans. Ecol. Environ.* **2017**, *226*, 559–569.

22. Peterson, M.L.; Gutkowski, R.M. Evaluation of the structural integrity of timber bridges. *NDT E Int.* **1999**, *32*, 43–48. [CrossRef]

23. Ross, R.J.; Pellerin, R.F.; Volny, N.; Salsig, W.W.; Falk, R.H. *Inspection of Timber Bridges Using Stress Wave Timing Nondestructive Evaluation Tools*; Report FPL-GTR; US Department of Agriculture, Forest Service, Forest Products Laboratory: Madison, WI, USA, 1999; p. 114.

24. Dackermann, U.; Crews, K.; Kasal, B.; Li, J.; Riggio, M.; Rinn, F.; Tannert, T. In situ assessment of structural timber using stress-wave measurements. *Mater. Struct.* **2014**, *47*, 787–803. [CrossRef]

25. Shao, J.; Wang, T.; Yin, H.; Yang, D.; Li, Y. Bolt looseness detection based on piezoelectric impedance frequency shift. *Appl. Sci.* **2016**, *6*, 298. [CrossRef]

26. Zou, D.; Liu, T.; Liang, C.; Huang, Y.; Zhang, F.; Du, C. An experimental investigation on the health monitoring of concrete structures using piezoelectric transducers at various environmental temperatures. *J. Intell. Mater. Syst. Struct.* **2015**, *26*, 1028–1034. [CrossRef]

27. Zou, D.; Liu, T.; Qiao, G.; Huang, Y.; Li, B. An experimental study on the performance of piezoceramic-based smart aggregate in water environment. *IEEE Sens. J.* **2014**, *14*, 943–944. [CrossRef]
28. Wang, D.; Song, H.; Zhu, H. Embedded 3D electromechanical impedance model for strength monitoring of concrete using a PZT transducer. *Smart Mater. Struct.* **2014**, *23*, 115019. [CrossRef]
29. Wang, D.; Zhang, J.; Zhu, H. Embedded electromechanical impedance and strain sensors for health monitoring of a concrete bridge. *Shock Vib.* **2015**, *2015*, 821395. [CrossRef]
30. Song, G.; Zhou, X.; Binienda, W. Thermal deformation compensation of a composite beam using piezoelectric actuators. *Smart Mater. Struct.* **2003**, *13*, 30. [CrossRef]
31. Song, G.; Qiao, P.Z.; Binienda, W.K.; Zou, G.P. Active vibration damping of composite beam using smart sensors and actuators. *J. Aerosp. Eng.* **2002**, *15*, 97–103. [CrossRef]
32. Song, G.; Gu, H. Active vibration suppression of a smart flexible beam using a sliding mode based controller. *J. Vib. Control* **2007**, *13*, 1095–1107. [CrossRef]
33. Wang, D.; Zhu, H. Monitoring of the strength gain of concrete using embedded PZT impedance transducer. *Constr. Build. Mater.* **2011**, *25*, 3703–3708. [CrossRef]
34. Wang, G. Analysis of bimorph piezoelectric beam energy harvesters using Timoshenko and Euler–Bernoulli beam theory. *J. Intell. Mater. Syst. Struct.* **2013**, *24*, 226–239. [CrossRef]
35. Caliò, R.; Rongala, U.B.; Camboni, D.; Milazzo, M.; Stefanini, C.; De Petris, G.; Oddo, C.M. Piezoelectric energy harvesting solutions. *Sensors* **2014**, *14*, 4755–4790. [CrossRef] [PubMed]
36. Venugopal, V.P.; Wang, G. Modeling and analysis of Lamb wave propagation in a beam under lead zirconatetitanate actuation and sensing. *J. Intell. Mater. Syst. Struct.* **2015**, *26*, 1679–1698. [CrossRef]
37. Lu, G.; Feng, Q.; Li, Y.; Wang, H.; Song, G. Characterization of Ultrasound Energy Diffusion Due to Small-Size Damage on an Aluminum Plate Using Piezoceramic Transducers. *Sensors* **2017**, *17*, 2796. [CrossRef] [PubMed]
38. Karaiskos, G.; Flawinne, S.; Sener, J.Y.; Deraemaeker, A. Design and validation of embedded piezoelectric transducers for damage detection applications in concrete structures. *Key Eng. Mater.* **2013**, *569*, 805–811. [CrossRef]
39. Hu, Y.; Yang, Y. Wave propagation modeling of the PZT sensing region for structural health monitoring. *Smart Mater. Struct.* **2007**, *16*, 706. [CrossRef]
40. Liu, T.; Huang, Y.; Zou, D.; Teng, J.; Li, B. Exploratory study on water seepage monitoring of concrete structures using piezoceramic based smart aggregates. *Smart Mater. Struct.* **2013**, *22*, 065002. [CrossRef]
41. Zhang, L.; Wang, C.; Song, G. Health status monitoring of cuplock scaffold joint connection based on wavelet packet analysis. *Shock Vib.* **2015**, *2015*, 695845. [CrossRef]
42. Feng, Q.; Kong, Q.; Jiang, J.; Liang, Y.; Song, G. Detection of Interfacial Debonding in a Rubber–Steel-Layered Structure Using Active Sensing Enabled by Embedded Piezoceramic Transducers. *Sensors* **2017**, *17*, 2001. [CrossRef] [PubMed]
43. Jiang, T.; Kong, Q.; Wang, W.; Huo, L.; Song, G. Monitoring of grouting compactness in a post-tensioning tendon duct using piezoceramic transducers. *Sensors* **2016**, *16*, 1343. [CrossRef] [PubMed]
44. Wang, T.; Song, G.; Wang, Z.; Li, Y. Proof-of-concept study of monitoring bolt connection status using a piezoelectric based active sensing method. *Smart Mater. Struct.* **2013**, *22*, 087001. [CrossRef]
45. Kong, Q.; Fan, S.; Bai, X.; Mo, Y.L.; Song, G. A novel embeddable spherical smart aggregate for structural health monitoring: Part I. Fabrication and electrical characterization. *Smart Mater. Struct.* **2017**, *26*, 095050. [CrossRef]
46. Kong, Q.; Fan, S.; Mo, Y.L.; Song, G. A novel embeddable spherical smart aggregate for structural health monitoring: Part II. Numerical and experimental verifications. *Smart Mater. Struct.* **2017**, *26*, 095051. [CrossRef]
47. Du, G.; Kong, Q.; Wu, F.; Ruan, J.; Song, G. An experimental feasibility study of pipeline corrosion pit detection using a piezoceramic time reversal mirror. *Smart Mater. Struct.* **2016**, *25*, 037002. [CrossRef]
48. Du, G.; Kong, Q.; Zhou, H.; Gu, H. Multiple cracks detection in pipeline using damage index matrix based on piezoceramic transducer-enabled stress wave propagation. *Sensors* **2017**, *17*, 1812. [CrossRef] [PubMed]
49. Yin, H.; Wang, T.; Yang, D.; Liu, S.; Shao, J.; Li, Y. A smart washer for bolt looseness monitoring based on piezoelectric active sensing method. *Appl. Sci.* **2016**, *6*, 320. [CrossRef]
50. Wang, B.; Huo, L.; Chen, D.; Li, W.; Song, G. Impedance-based pre-stress monitoring of rock bolts using a piezoceramic-based smart washer—A feasibility study. *Sensors* **2017**, *17*, 250. [CrossRef] [PubMed]

51. Song, G.; Li, W.; Wang, B.; Ho, S.C.M. A review of rock bolt monitoring using smart sensors. *Sensors* **2017**, *17*, 776. [CrossRef] [PubMed]

52. Huo, L.; Wang, B.; Chen, D.; Song, G. Monitoring of Pre-Load on Rock Bolt Using Piezoceramic-Transducer Enabled Time Reversal Method. *Sensors* **2017**, *17*, 2467. [CrossRef] [PubMed]

53. Xu, J.; Hao, J.; Li, H.; Luo, M.; Guo, W.; Li, W. Experimental Damage Identification of a Model Reticulated Shell. *Appl. Sci.* **2017**, *7*, 362. [CrossRef]

54. Kong, Q.; Robert, R.H.; Silva, P.; Mo, Y.L. Cyclic crack monitoring of a reinforced concrete column under simulated pseudo-dynamic loading using piezoceramic-based smart aggregates. *Appl. Sci.* **2016**, *6*, 341. [CrossRef]

55. Kong, Q.; Feng, Q.; Song, G. Water presence detection in a concrete crack using smart aggregates. *Int. J. Smart Nano Mater.* **2015**, *6*, 149–161. [CrossRef]

56. Park, G.; Farrar, C.R.; di Scalea, F.L.; Coccia, S. Performance assessment and validation of piezoelectric active-sensors in structural health monitoring. *Smart Mater. Struct.* **2006**, *15*, 1673. [CrossRef]

57. Wu, F.; Chan, H.L.; Chang, F.K. Ultrasonic guided wave active sensing for monitoring of split failures in reinforced concrete. *Struct. Health Monit.* **2015**, *14*, 439–448. [CrossRef]

58. Kim, S.D.; In, C.W.; Cronin, K.E.; Sohn, H.; Harries, K. Reference-free NDT technique for debonding detection in CFRP-strengthened RC structures. *J. Struct. Eng.* **2007**, *133*, 1080–1091. [CrossRef]

59. Kessler, S.S.; Spearing, S.M.; Soutis, C. Damage detection in composite materials using Lamb wave methods. *Smart Mater. Struct.* **2002**, *11*, 269. [CrossRef]

60. Kong, Q.; Hou, S.; Ji, Q.; Mo, Y.L.; Song, G. Very early age concrete hydration characterization monitoring using piezoceramic based smart aggregates. *Smart Mater. Struct.* **2013**, *22*, 085025. [CrossRef]

61. Kong, Q.; Song, G. A comparative study of the very early age cement hydration monitoring using compressive and shear mode smart aggregates. *IEEE Sens. J.* **2017**, *17*, 256–260. [CrossRef]

62. Xu, K.; Kong, Q.; Chen, S.; Song, G. Early Determination of the Presence of Low Strength Concrete in Reinforced Concrete Beam-Column Joints Using Piezoceramic-Based Transducers. *IEEE Sens. J.* **2017**, *17*, 3244–3250. [CrossRef]

63. Lim, Y.Y.; Kwong, K.Z.; Liew, W.Y.H.; Soh, C.K. Non-destructive concrete strength evaluation using smart piezoelectric transducer—A comparative study. *Smart Mater. Struct.* **2016**, *25*, 085021. [CrossRef]

64. Cuc, A.; Giurgiutiu, V. Disbond detection in adhesively bonded structures using piezoelectric wafer active sensors. In *Health Monitoring and Smart Nondestructive Evaluation of Structural and Biological Systems III*; International Society for Optics and Photonics: Bellingham, WA, USA, 2004.

65. Roth, W.; Giurgiutiu, V. Adhesive disbond detection using piezoelectric wafer active sensors. In *Structural Health Monitoring and Inspection of Advanced Materials, Aerospace, and Civil Infrastructure 2015*; International Society for Optics and Photonics: Bellingham, WA, USA, 2015.

66. Park, D.Y.; Joe, D.J.; Kim, D.H.; Park, H.; Han, J.H.; Jeong, C.K.; Park, H.; Park, J.G.; Joung, B.; Lee, K.J. Self-Powered Real-Time Arterial Pulse Monitoring Using Ultrathin Epidermal Piezoelectric Sensors. *Adv. Mater.* **2017**, *29*, 1702308. [CrossRef] [PubMed]

67. Jeong, C.K.; Han, J.H.; Palneedi, H.; Park, H.; Hwang, G.T.; Joung, B.; Kim, S.G.; Shin, H.J.; Kang, I.S.; Ryu, J.; et al. Comprehensive biocompatibility of nontoxic and high-output flexible energy harvester using lead-free piezoceramic thin film. *APL Mater.* **2017**, *5*, 074102. [CrossRef]

68. Sun, Z.; Chang, C.C. Structural damage assessment based on wavelet packet transform. *J. Struct. Eng.* **2002**, *128*, 1354–1361. [CrossRef]

69. Song, G.; Li, H.; Gajic, B.; Zhou, W.; Chen, P.; Gu, H. Wind turbine blade health monitoring with piezoceramic-based wireless sensor network. *Int. J. Smart Nano Mater.* **2013**, *4*, 150–166. [CrossRef]

70. Asgarian, B.; Aghaeidoost, V.; Shokrgozar, H.R. Damage detection of jacket type offshore platforms using rate of signal energy using wavelet packet transform. *Mar. Struct.* **2016**, *45*, 1–21. [CrossRef]

71. Jiang, T.; Kong, Q.; Patil, D.; Luo, Z.; Huo, L.; Song, G. Detection of debonding between fiber reinforced polymer bar and concrete structure using piezoceramic transducers and wavelet packet analysis. *IEEE Sens. J.* **2017**, *17*, 1992–1998. [CrossRef]